

Chain Length Dependent Termination Rate Coefficients of Methyl Methacrylate (MMA) in the Gel Regime: Accessing $k_t^{i,i}$ Using Reversible Addition-Fragmentation Chain Transfer (RAFT) Polymerization

Geoffrey Johnston-Hall,[†] Martina H. Stenzel,[‡] Thomas P. Davis,[‡] Christopher Barner-Kowollik,[‡] and Michael J. Monteiro^{*,†}

Australian Institute of Bioengineering and Nanotechnology, School of Molecular and Microbial Sciences, University of Queensland, Brisbane QLD 4072, Australia, and Centre for Advanced Macromolecular Design, School of Chemical Sciences and Engineering, the University of New South Wales, Sydney, NSW 2052, Australia

Received October 19, 2006; Revised Manuscript Received January 21, 2007

ABSTRACT: The termination rate coefficient, $k_t^{i,i}$, for propagating chains of near equal length, i , was evaluated using the RAFT–CLD–T method over a wide range of chain lengths and up to a conversion of 70% for MMA polymerizations carried out in the presence of the RAFT agent, CPDB, at 80 °C. We found that the conversion for the gel onset corresponded to the conversion at which polymer chains begin to overlap (i.e., c^*), and was found to range from 15 to 30% conversion depending on the M_n . It was further shown that c^* also corresponded with the gel onset conversions for vinyl acetate and methyl acrylate. The chain length dependence of k_t in the gel regime scaled as $\alpha_{\text{gel}}(x) = 1.8x + 0.056$, suggesting that reptation alone does not play a role in our system. A composite model was then derived to accurately describe $k_t^{i,i}$ for chain lengths up to 3200 and conversions up to 70%. The $k_t^{i,i}$ profiles for well-known termination models were tested and most gave unsatisfactory agreement with our experiments. Our model can be readily applied to any monomer provided accurate $k_t^{i,i}(x)$ data can be determined.

Introduction

The gel effect observed in free-radical polymerization (FRP) has been intensively investigated since the original observations by Schultz¹ and Trommsdorf.² The onset of the gel effect is observed from the sudden rise in the rate of polymerization (R_p) as a result of an increased propagating radical concentration due to the decreased average termination rate coefficient, $\langle k_t \rangle$. The slow rate for the diffusion of the polymeric radicals to terminate with each other has been used to explain this phenomenon.^{3,4} Diffusion is dependent on many factors such as solution viscosity,⁵ chain length,⁶ polymer coil dimensions,⁷ polymer–solvent interactions,⁸ and intra- and intermolecular interactions between polymer chains.⁹ In this study, we address an important question: Is the gel onset controlled by physical interactions between the polymer radicals and the polymer matrix, and can this be quantified and incorporated into a kinetic termination model?

Most termination models to date have been based on broad radical chain length distributions, and have determined the termination coefficient ($k_t^{i,j}$) between two radicals of different chain lengths, i and j , from an average of $k_t^{i,i}$ and $k_t^{j,j}$. The problem with all these model approaches is that accurate determination of $k_t^{i,i}$ and $k_t^{j,j}$ and their dependence on conversion (see eq 1)¹⁰ cannot be accurately obtained, and thus adjustable parameters are used in the models to provide a fit with experimental rate and molecular weight data. In addition, the

change over from dilute to the gel regime (i.e., the onset of the gel effect) in most models is based on empirical data rather than any physical representation.

$$k_t^{i,i} = k_t^{1,1} i^{-\alpha} \quad (1)$$

Equation 1 evaluates $k_t^{i,i}$ using $k_t^{1,1}$ (the termination rate coefficient between two monomeric radicals) and α , which relates the dependence of chain length to termination. This chain length dependence has previously been evaluated using a variety of experimental, theoretical and model dependent procedures.¹¹

Recently, the model independent reversible addition–fragmentation chain transfer CLD termination (RAFT–CLD–T) method introduced by Barner-Kowollik and co-workers¹² has allowed the accurate determination of $k_t^{i,i}$ (and potentially $k_t^{i,j}$)¹³ values for a variety of polymers over a wide range of chain lengths by combining accurate R_p measurements with eq 2¹⁴ and evaluating the evolution of molecular weight, M_n , with conversion, x , according either to the theoretical molecular weight evolution described by eq 3,¹⁵ or through the experimental M_n data.

$$\langle k_t \rangle(t) = \frac{d \left(\frac{R_p(t)}{k_p([M]_0 - \int_0^t R_p(t) dt)} \right)}{2 \left(\frac{R_p(t)}{k_p([M]_0 - \int_0^t R_p(t) dt)} \right)^2} \quad (2)$$

$$i = \frac{[M]_0 x}{([RAFT]_0 - [RAFT]_x) + g/([I]_0 - [I]_x)} \quad (3)$$

* Author to whom correspondence should be sent. E-mail: m.monteiro@uq.edu.au.

[†] Australian Institute of Bioengineering and Nanotechnology, School of Molecular and Microbial Sciences, University of Queensland.

[‡] Centre for Advanced Macromolecular Design, School of Chemical Sciences and Engineering, The University of New South Wales.

where $[M]_0$ is the initial monomer concentration, x is fractional monomer conversion to polymer, $[RAFT]_0$ is the initial RAFT agent concentration, $[RAFT]_x$ is RAFT agent concentration at x , a is the mode of termination (a equals 1 for termination by combination and 2 for disproportionation), $[I]_0$ is the initial initiator concentration, $[I]_x$ is initiator concentration at x , k_d is the initiator decomposition rate coefficient, k_p is the propagation rate coefficient, and f is the initiator efficiency.

The RAFT-CLD-T method has since been applied to a range of monomer systems, including various acrylates^{16–18} and vinyl acetate.¹⁹ In addition, we have recently shown that for methyl methacrylate (MMA) polymerizations in dilute solutions (i.e., below the onset of the gel effect) using the RAFT-CLD-T method,²⁰ the $k_t^{i,i}$ data fit a composite model describing “short” chain length and “long” chain length regimes in agreement with earlier studies.²¹ The value of α in the “short” region, α_S (when $i < 100$, below the crossover point from short to long termination, i_{SL}), was equal to 0.65, and for chains greater than 100, a value of 0.15 for α_L was determined. In a further refinement, Barner-Kowollik and co-workers have used the RAFT-CLD-T method to determine $k_t^{i,i}$ for methyl acrylate²² and vinyl acetate¹⁹ up to 80% conversion, in which the gel effect is not as pronounced as for MMA. The $k_t^{i,i}$ values reported in these studies support the widely accepted view that k_t scales according to two major regimes up to 80% conversion; the dilute solution and gel regimes, where chain length dependent exponents greater than 1 are common in the gel regime. However, the problem remains that no physical model has yet adequately described the transition between these regimes (i.e., the gel onset). Among the many physical representations used to describe the gel onset, the following two have been the most widely employed and debated: (1) overlap of the polymer chains and the onset of entanglements,²³ and (2) restricted mobility of the polymer chains due to a decreased free volume.²⁴ Studies using conventional FRP have attempted to find some distinct correlation between the gel onset and these two physical models,²⁵ but none have to date proven successful.

In this work, we use the RAFT-CLD-T method for bulk MMA polymerizations to explore the physical polymer interactions at the gel onset. MMA was chosen since there is a pronounced polymerization rate increase in the gel regime, and as such is an ideal model system to explore the physical aspects of polymer interactions in the gel. The chain length dependent termination coefficient, $k_t^{i,i}$, over a wide range of chain lengths up to 70% conversion will be evaluated, and will be compared with various models in the literature. We will then provide a semiempirical model based on polymer interactions at the gel onset to be used in the future to predict “living” and conventional free-radical polymerizations over the full conversion range.²⁶ We have not determined $k_t^{i,i}$ in the glass regime because many of the parameters (e.g., k_p , f , k_d) that are used in eq 2 are no longer considered constant.

Experimental Section

Chemicals. Methyl methacrylate (MMA, 99%, Aldrich) was purified by filtration through basic alumina (70–230 mesh) to remove inhibitors prior to use. 2,2'-azobis(isobutyronitrile) (AIBN, 99%, DuPont) was purified by recrystallization from methanol. 2-Cyanoprop-2-yl dithiobenzoate (CPDB) was prepared according to the literature procedure.²⁰

A Typical Procedure for the RAFT Polymerization of MMA. MMA monomer (2 mL, 9.34 mol/L), AIBN (0.00067 g, 2.01 mmol/L), and CPDB (0.00440 g, 9.93 mmol/L) were added to a reaction vessel, degassed by four successive freeze–pump–thaw cycles, and polymerized at 80 °C. Conversion was measured gravimetrically

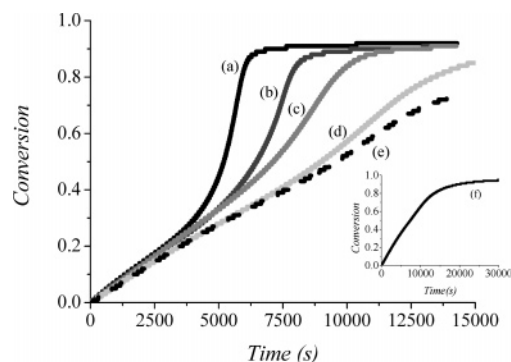


Figure 1. Fractional monomer conversion vs time profiles for the cyanoisoprop-2-yl dithiobenzoate (CPDB) mediated polymerization of methyl methacrylate (MMA, 9.34 M) at 80 °C using azobis(isobutyronitrile) (AIBN, ~2 mM). The concentrations of CPDB used are (a) 0, (b) 2.13, (c) 4.98, (d) 9.93, and (e) 19.9 mM. Inset: (f) 54.4 mM CPDB, and 8.83 mM AIBN mediated bulk polymerization of MMA (9.34 M) at 80 °C.

by drying the samples in a vacuum oven at ambient temperature until at constant weight, and the molecular weight distribution was determined by size exclusion chromatography.

A Typical Differential Scanning Calorimetry (DSC) RAFT Polymerization of MMA. DSC polymerizations were all performed in duplicate. MMA monomer (2 mL, 9.34 M), AIBN (0.00067 g, 2.01 mM), and CPDB (0.00440 g, 9.93 mM) were added to a reaction vessel, degassed by four successive freeze–pump–thaw cycles and transferred into gastight DSC pans in a glove bag under nitrogen. The sample weights in the DSC pans ranged between 30 and 60 mg. (The weight in the DSC pans was measured by mass difference between empty and full.) The polymerizations were carried out isothermally at 80 °C, and the heat of polymerization measured by comparing the heat flow from the polymerization pan and an empty pan on a Perkin-Elmer DSC 7 with a TAC 7/DX thermal analysis instrument controller. The DSC instrument was calibrated with a standard indium sample of known mass, melting point temperature and associated enthalpy change. The rate of polymerization (R_p) and monomer conversions (x) were calculated using literature values for the heat of polymerization of MMA ($\Delta H_p = -52.8 \text{ kJ mol}^{-1}$).²⁷

Size Exclusion Chromatography. Size exclusion chromatography (SEC) measurements were performed using a Waters Alliance 2690 Separations Module equipped with an autosampler, column heater, differential refractive index detector and a photodiode array (PDA) connected in series. HPLC grade tetrahydrofuran was used as eluent at a flow rate of 1 mL min⁻¹. The columns consisted of three 7.8 × 300 mm Waters Styragel GPC columns connected in series, comprising 2 linear UltraStyragel and one Styragel HR3 columns. Polymethyl methacrylate standards ranging from 2000000 to 540 g mol⁻¹ were used for calibration.

Calculation Methods. The three-dimensional surface fitting was performed on experimental $\log k_t$ vs $\log i$ vs x data using the software package TableCurve 3D. The individual effects of chain length and conversion on termination at conversions beyond the gel effect were subsequently separated by extraction of $\log k_t$ profiles at stationary values of either i , or x .²²

Results and Discussion

The RAFT agent, CPDB, gave reasonable control of M_n and polydispersity (PDI) for the living radical polymerization of MMA (see “Supporting Information”) and thus provides an appropriate means for evaluating the chain length dependent termination rate coefficient $k_t^{i,i}$ for this monomer.²⁰ The effect of increasing the CPDB concentration up to 20 mM on the rate of polymerization of MMA in bulk at 80 °C is given in Figure 1. In all polymerizations, the AIBN concentration was kept constant (see Table 2 for experimental conditions). The conver-

Table 1. Kinetics Parameters Used for Analysis of $k_t^{i,i}$ from the RAFT-Mediated Polymerization of Methyl Methacrylate (MMA) at 80 °C in Bulk, Initiated with Azobis(isobutyronitrile) (AIBN) in the Presence of Cyanoisoprop-2-yl Dithiobenzoate (CPDB)

T (°C)	k_p (L mol ⁻¹ s ⁻¹)	k_d (s ⁻¹)	f	ΔH_p (kJ mol ⁻¹)
80	1332 ⁷⁸	1.1×10^{-4} ¹⁶	0.70 ⁷⁹	-52.8 ²⁷

Table 2. Determination of the Conversion (x) and M_n at the Onset of the Gel Effect for the Bulk Polymerization of Methyl Methacrylate (MMA) at 80 °C, Initiated with Azobis(isobutyronitrile) (AIBN) in the Presence of Cyanoisoprop-2-yl Dithiobenzoate (CPDB)

expt	[CPDB] ₀ (mM)	[AIBN] ₀ (mM)	method 1		method 2	
			$x_{\text{gel-onset}}$	$M_{n,\text{gel-onset}}$	$x_{\text{gel-onset}}$	$M_{n,\text{gel-onset}}$
1	0	2.01				
2	2.13	2.01	0.14	73 150	0.275	130 300
3	4.98	1.99	0.17	40 590	0.29	61 240
4	9.93	2.01	0.20	27 560	0.30	42 100
5	19.9	2.28	0.26	15 630	0.37	22 600
6	54.4	8.83	0.33	7020	0.43	10 310

sion (x) vs time profiles for all polymerizations were similar up to 2500 s and approximately 20% conversion. This result supports the argument that CPDB does not retard or influence the polymerization rate²⁸ through either intermediate radical termination^{15,29–32} or slow fragmentation,^{33–35} and allows for a quantitative analysis of $k_t^{i,i}$ to be obtained. At times greater than 2500 s (or >20% conversion) there was a dramatic increase in R_p , characteristic of the onset of the gel effect, which is most clearly observed for the polymerization without CPDB. The point at which R_p increased is denoted as the gel onset ($x_{\text{gel-onset}}$), and from Figure 1 it was found that at higher concentrations of CPDB, $x_{\text{gel-onset}}$ increased to greater conversions and polymerization times.

Time-dependent termination rate coefficients, $\langle k_t \rangle(t)$, were calculated from accurate R_p data according to eq 2 and using the parameters given in Table 1. A three-dimensional plot of $\log k_t^{i,i}$ as a function of both conversion and chain length i was constructed and fitted with a surface function (Figure 2). The Fourier series polynomial surface function (see “Supporting Material”) gave an excellent fit to the data with a correlation coefficient close to 1 ($r^2 > 0.99$). Under dilute conditions (below 20% conversion) $k_t^{i,i}$ was only slightly dependent on x for chain lengths obtained between 10 and 1000. The graph showed that both chain length and conversion influenced $k_t^{i,i}$; the greater the chain length or conversion the lower the value of $k_t^{i,i}$. A more detailed discussion of the dependencies of $k_t^{i,i}$ on conversion and i will be given below. The graph also showed that the $k_t^{i,i}$ topology decreased rapidly after approximately 20% conversion for chain lengths of approximately 1000, and approximately 50% conversion for chain lengths of approximately 10.

Determination of $x_{\text{gel-onset}}$ for each experiment was evaluated according to two methods. Method 1 used the initial change in linearity observed in the plot of $\log k_t^{i,i}$ vs $\log x$, and method 2 evaluated $x_{\text{gel-onset}}$ as the conversion at which the dilute and gel regions intersected (see Figure 3). Table 2 gives the values of $x_{\text{gel-onset}}$ determined from both methods, and the functions with respect to M_n are given in eq 4, parts a and b. These relationships show that the conversion for the gel onset decreased as M_n increased, suggesting that when targeting higher molecular weights in a RAFT polymerization faster rates of polymerization will be observed, which is consistent with previous findings³⁶ and the data presented in Figure 2.

$$x_{\text{gel-onset}}(\text{method 1}) = 12.0 M_n^{-0.399} \quad (4a)$$

$$x_{\text{gel-onset}}(\text{method 2}) = 2.628 M_n^{-0.21} \quad (4b)$$

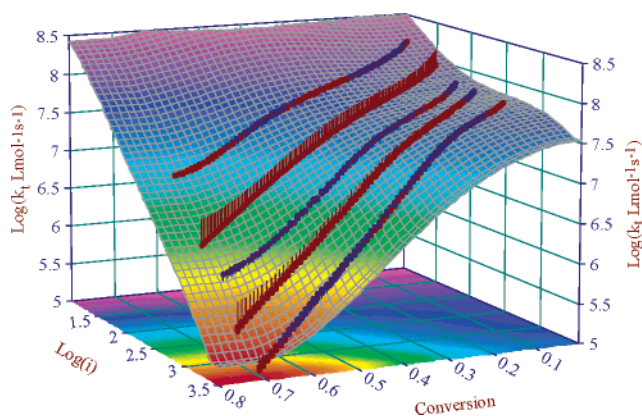


Figure 2. Three-dimensional plot of the termination rate coefficients, k_t 's, for RAFT-mediated methyl methacrylate (MMA) polymerized in bulk and in the presence of cyanoisoprop-2-yl dithiobenzoate (CPDB), initiated with AIBN at 80 °C. The data was fit with a surface plot using the TableCurve 3D software ($r^2 > 0.99$). Drop lines indicate some minor deviation from the surface fit function.

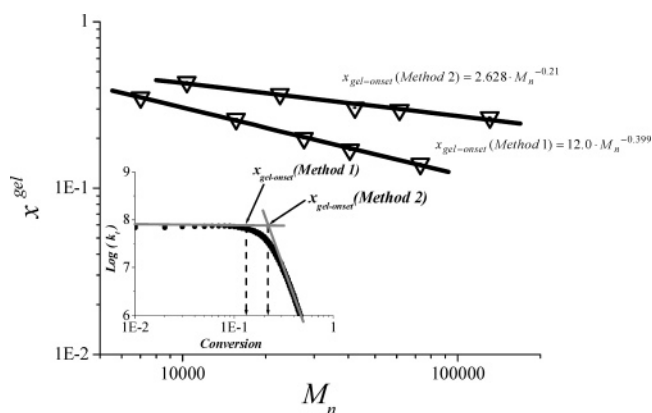


Figure 3. Determination of the gel onset conversion ($x_{\text{gel-onset}}$) using the initial change in slope of $k_t^{i,i}$ (method 1) and the intersection between dilute and gel regimes (method 2). This data was derived from the surface function in Figure 2.

There has been rigorous debate in defining $x_{\text{gel-onset}}$ in terms of a physical model. Trommsdorff² suggested that the gel onset was the result of large changes in the bulk solution viscosity, causing a sudden and significant reduction in diffusion of polymeric radicals. However, after comparison of the polymerization kinetics for different acrylates and methacrylates, a number of groups concluded that bulk viscosity changes alone did not provide an adequate explanation for the rate determining factor in termination.^{37,38}

Balke and Hamielec²⁴ proposed free volume to explain the onset of the gel effect, based on Mita and Kambe's³⁹ successful description of the “glass” effect using free volume theory. However, free volume theory does not account for chain length effects. Around the same time, O'Driscoll^{23,40,41} proposed that the gel onset coincided with the formation of chain entanglements.^{42–45} Following from this concept, Turner et al.^{8,46–49} suggested that $x_{\text{gel-onset}}$ could be identified with polymer chain overlap (c^*), a concept that was also proposed by Tulig and Tirrell.^{50,51} For example, exponent values determined for conventional FRP include -0.24 ,⁵⁰ ~ 0.325 ,⁴⁷ 0.29 ,²⁵ and -0.5 ,^{52,53} which are in general agreement with our observations (eq 4, parts a and b). Cotton et al.⁵⁴ suggested that in fact c^* was not a sharp transition but gradually changed since the radius of gyration (R_g) was not constant under dilute conditions. They therefore suggested that c^* falls between an upper (eq 5a) and lower (eq 5b) limit.⁵⁴

$$c_{\max}^* = \frac{M_n}{R_g^3 N_A} \quad (5a)$$

$$c_{\min}^* = \frac{3}{4\pi} \frac{M_n}{R_g^3 N_A} \quad (5b)$$

where N_A is Avogadro's constant. The radius of gyration, R_g , may be calculated using⁵⁵

$$R_g^2 = \frac{C^\infty M_n l^2}{mw} \quad (6)$$

where mw is the molecular weight of monomer, l the length between two monomer units, and C^∞ is the expansion factor. This proposal is supported from our work (Figure 3) as shown from the gradual changeover in $k_t^{i,i}$ over approximately 5% conversion from dilute to gel regimes. Figure 4A compares the theoretical profiles for c_{\min}^* and c_{\max}^* (calculated for MMA using $mw = 100.21 \text{ g mol}^{-1}$, $l = 2 \times 1.54 \text{ \AA}$,⁵⁶ and $C^\infty = 7^{56}$) and the experimental $x_{\text{gel-onset}}$ curves determined from methods 1 and 2 (see eq 4, parts a and b). There is excellent agreement between $x_{\text{gel-onset}}$ determined by method 1 and c_{\max}^* (eq 5a) as shown in curves a and d, respectively. Excellent agreement was also found between the molecular weight power law dependence of $x_{\text{gel-onset}}$ (proportional to $M_n^{-0.399}$ —method 1, eq 4a) and c_{\max}^* for MMA (proportional to $M_n^{-0.37}$ —Table 3).⁵⁷

Subsequent analysis of the $k_t^{i,i}(x)$ data for methyl acrylate²² (MA) and vinyl acetate¹⁹ (VAc) polymerizations also showed good agreement between c^* (theory) and $x_{\text{gel-onset}}$ determined by method 1 (See "Supporting Material" for the figures for c^* for MA and VAc). Most encouraging was that the form of both $x_{\text{gel-onset}}$ and c_{\max}^* curves for all monomers is similar.

The M_n 's determined experimentally for each polymerization are also given in Figure 4B, which were in excellent agreement with theory (using $C_{\text{tr,RAFT}} = 15.2^{20}$). It can be seen that as the targeted molecular weight (at 100% conversion) in a "living" radical polymerization was decreased the onset of the gel effect was extended to greater conversions. The data suggests that the gel effect will be eliminated for short chains of $i < 30$, and for chain lengths greater than this value, a gel effect will always occur regardless of the experimental conditions used. It should be emphasized, however, that these observations do not indicate that for all $i > 30$ the characteristic increase in R_p associated with the gel effect will be observed. As R_p is proportional to $\langle k_t \rangle^{-0.5}$ only a significant decrease in $\langle k_t \rangle$ will lead to an observable R_p increase. Hence, the bulk polymerization of MMA (9.34 M) in the presence of 54.4 mM CPDB and 8.83 mM AIBN at 80 °C resulted in no observable R_p increase (curve f, Figure 1), despite a clear decrease found in the $\langle k_t^{i,i} \rangle$ profile (curve e, Figure 6). This last point is also consistent with the use of chain transfer agents in conventional FRP to control the magnitude of autoacceleration by decreasing $\langle M_n \rangle$.⁵⁸

In the gel regime, the effect of $k_t^{i,i}$ as a function of i at various conversions was determined using the surface function obtained from the fit in Figure 2. Figure 5 shows that although $k_t^{i,i}$ is affected by chain length, a more pronounced effect comes from the change in conversion. A chain length dependent power law exponent, $\alpha_{\text{gel}}(x)$, is determined from the slope in the gel region, and plotted as a function of conversion (see inset in Figure 5) with the following linear relationship:

$$\alpha_{\text{gel}}(x) = 1.8x + 0.056 \quad (7)$$

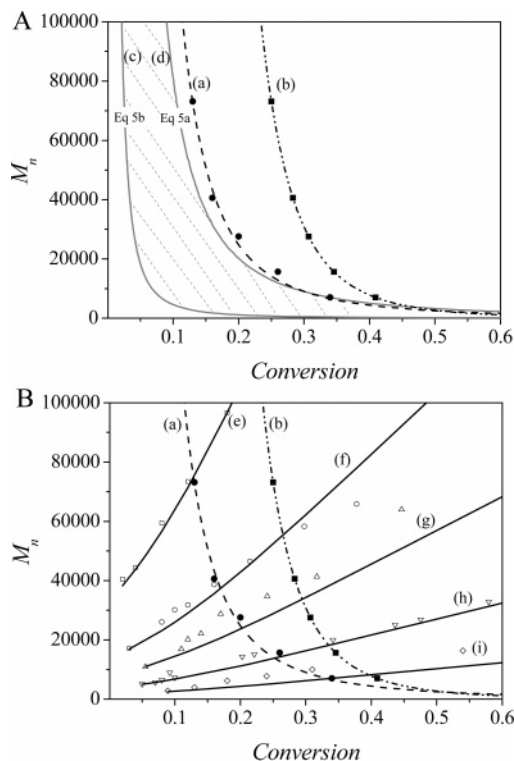


Figure 4. Bulk polymerizations of methyl methacrylate (MMA, 9.34 M) at 80 °C using azobis(isobutyronitrile) (AIBN) in the presence of cyanoisoprop-2-yl dithiobenzoate (CPDB). (A) Gel onset point ($x_{\text{gel-onset}}$) determined from methods 1 and 2, and c_{\max}^* and c_{\min}^* determined from eq 5, parts a and b. (B) M_n vs conversion profiles. Curve a represents the experimental $x_{\text{gel-onset}}$ determined by method 1, curve b the experimental $x_{\text{gel-onset}}$ determined by method 2, curve c the c_{\min}^* determined using eq 5b, and curve d the c_{\max}^* determined using eq 5a. Polymerizations were carried out using the following CPDB concentrations: (e) 2.13, (f) 4.98, (g) 9.93, (h) 19.9, and (i) 54.4 mM. The solid lines represent $M_{n,\text{theory}}$ using eq 3 and $C_{\text{tr,RAFT}} = 15.2^{20}$. The shaded area (Figure 4A) represents the limits between c_{\min}^* and c_{\max}^* .

and can be combined with eq 1 to give

$$k_t^{i,i} \propto i^{-(1.8x + 0.056)} \quad (8)$$

It has been claimed that diffusion in the gel regime is through reptation with a dependence of i^{-2} (Table 3).^{50,51,59} From eq 7, $\alpha_{\text{gel}}(x)$ will approach 2 only at limiting values of x coinciding with the glass regime. Inconsistencies have also been observed between reptation and self-diffusion coefficients.⁶⁰ It should be noted that this does not mean that reptation does not occur but that the polymeric radicals are additionally controlled by other diffusion processes. Unfortunately, attempts to compare $\alpha_{\text{gel}}(x)$ with other theoretical models did not prove fruitful (see Table 3).

Given that no physical model is adequately able to describe the gel regime, we developed a semiempirical model to describe $k_t^{i,i}(x)$ both in the dilute and gel regimes using a similar methodology to that recently described by Smith et al.²¹ We previously found this approach effective in describing $k_t^{i,i}$ in the dilute solution regime for MMA,²⁰ but have in this work extended the model to describe termination in the gel regime up to the glass regime. To describe $k_t^{i,i}(x)$ in these two regimes the following expressions were used along with the parameters given in Table 4.

Table 3. Theoretically Predicted and Experimentally Observed Scaling Laws for Poly(methyl Methacrylate) (PMMA)

quantity	prediction	ref	found	ref
bulk viscosity	$\eta(\Theta) \propto M^{0.5}$	80	$\eta \propto M^{0.68}$	81
dilute solutions	$\eta(\text{good}) \propto M^{0.8}$	80	$\eta \propto M^b, b \sim 3.0-7.0$	81
concentrated solutions	$\eta \propto M^{3.0}$	82	$D_s \propto M^{-(2.02\alpha + 0.664)}$	83
	$\eta \propto M^{3.4}$	80		
self diffusion	$D_s(\text{bulk}) \propto M^{-2.0}$	82, 84, 85		
(reptation)	$D_s(\text{soln}) \propto M^{-2.0}c^{-7/4}$	82, 84, 85		
overlap concentration	$c^* \propto M^{-0.5}$	86	$c^* \propto M^{-0.37}$	57
(random coil)			$c^* \propto M^{-0.399}$	this work
radius of gyration	$R_g \propto M^{0.5}$	55	$R_g \propto M^{0.56}$	87
(random coil)				
correlation length	$\xi \propto M^0$	50		
termination rate coeff	$k_t \propto M^{-1.5}$	88		
(entangled melts)				

Dilute Solution Regime, for $i < i_{\text{gel}}$

$$\text{for } i_x < i_{\text{SL}}, \quad k_t^{i,i} = k_t^{1,1} i_x^{-\alpha_S} \quad (9)$$

$$\text{for } i_x \geq i_{\text{SL}}, \quad k_t^{i,i} = k_t^{1,1} i_{\text{SL}}^{\alpha_L - \alpha_S} i_x^{-\alpha_L} \quad (10)$$

Gel Regime, for $i \geq i_{\text{gel}}$

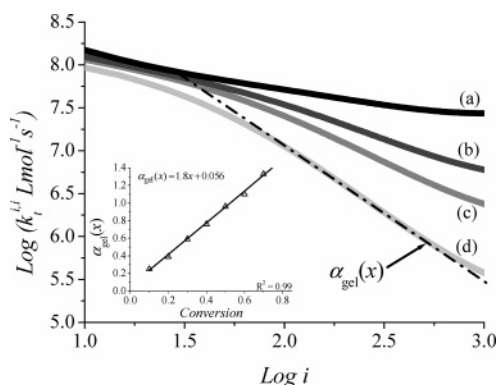
$$\text{for } i_x < i_{\text{SL}}, \quad k_t^{i,i} = k_t^{1,1} i_{\text{gel}}^{\alpha_{\text{gel}}(x) - \alpha_S} i_x^{-\alpha_{\text{gel}}(x)} \quad (11)$$

$$\text{for } i_x \geq i_{\text{SL}}, \quad k_t^{i,i} = k_t^{1,1} i_{\text{SL}}^{\alpha_L - \alpha_S} i_{\text{gel}}^{\alpha_{\text{gel}}(x) - \alpha_L} i_x^{-\alpha_{\text{gel}}(x)} \quad (12)$$

where i_{SL} represents the cross over chain length from short to long in dilute solution, α_S is the chain length dependent power law exponent for short chains in dilute solution, α_L is the chain length dependent power law exponent for long chains in dilute solution,²⁰ and i_{gel} represents the cross over chain length from dilute solution to the gel regime.

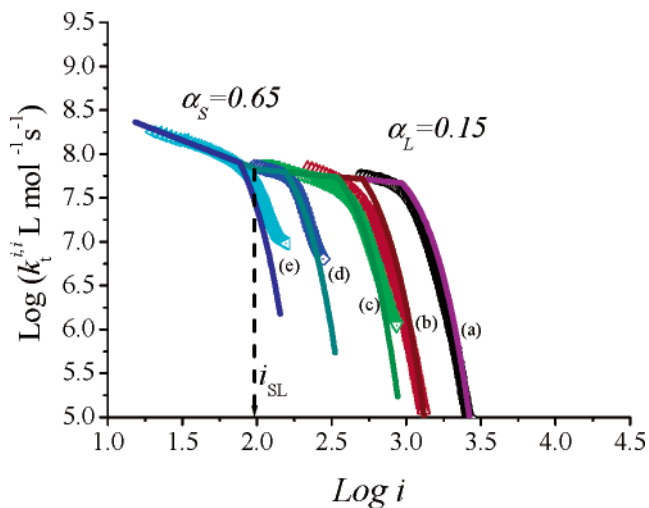
To validate this approach, model predictions were compared to experimentally determined $k_t^{i,i}$ profiles found for a series of experiments describing $k_t^{i,i}$ over a wide range of chain lengths and up to 70% conversion (Figure 6). Agreement between the model and experiment was excellent for the entire conversion range of 5–70% and for chain lengths of 10–3000. Initially, the expression for $x_{\text{gel-onset}}$ (method 1, eq 4a) was used to describe i_{gel} in the model and gave excellent agreement with experimental $k_t^{i,i}$ profiles. However, subsequent computational kinetic simulations (not shown)²⁶ indicated $x_{\text{gel-onset}}$ using method 2 (eq 4b) was more accurate in fitting the rates of polymerization and molecular weight data for both conventional FRP and “living” radical polymerization up to high conversions.

A feature of this model is the gradual transition from dilute solution to gel regimes through the implementation of conversion dependent functions for both $i_{\text{gel-onset}}$ and $\alpha_{\text{gel}}(x)$. Our

**Figure 5.** $\log k_t$ vs $\log i$, profiles extracted from the $k_t^{i,i}(x)$ surface fit function determined at (a) 20% conversion, (b) 40% conversion, (c) 50% conversion, and (d) 70% conversion.**Table 4. Parameters Used in the “Composite” Model to Describe $k_t^{i,i}(x)$ for the Polymerization of Methyl Methacrylate (MMA) at 80 °C^a**

parameter	value
$k_t^{1,1}$	1.2×10^9
α_S	0.65
i_{SL}	100
α_L	0.15
i_{gel}	$\left(\frac{x}{2.628}\right)^{-1/0.21}$
$\alpha_{\text{gel}}(x)$	$\frac{\text{mw}}{\text{mw}}$ $\alpha_{\text{gel}}(x) = 1.8x + 0.056$ (eq 7)

^aValues were taken from this work and ref 20.

**Figure 6.** Comparison between “composite” model and experiment for the change in $\langle k_t^{i,i} \rangle$ with i for bulk polymerizations of methyl methacrylate (MMA) in the presence of cyanoisoprop-2-yl dithiobenzoate (CPDB) initiated with azobis(isobutyronitrile) (AIBN) at 80 °C. Solid lines represent composite model. Key: (a) [CPDB] = 2.13 mM and [AIBN] = 2.01 mM; (b) [CPDB] = 4.98 mM and [AIBN] = 1.99 mM; (c) [CPDB] = 9.93 mM and [AIBN] = 2.01 mM; (d) [CPDB] = 19.9 mM and [AIBN] = 2.28 mM; (e) [CPDB] = 54.4 mM and [AIBN] = 8.83 mM.

model, therefore, presents an accurate fit of termination rate coefficients as a function of both conversion and chain length. Importantly, one of the main motivations for developing this composite or semiempirical model strategy is its “universal” nature. This model approach can be readily applied to any monomer provided accurate $k_t^{i,i}(x)$ data can be accessed and parameters $k_t^{1,1}$, α_S , i_{SL} , α_L , i_{gel} , and $\alpha_{\text{gel}}(x)$ evaluated.

The elucidation of $k_t^{i,i}$ profiles as a function of conversion and chain length allow us to compare the various models proposed in the literature to our experimental data. Most termination models have been developed to describe broad radical chain length distributions in conventional FRP, and have

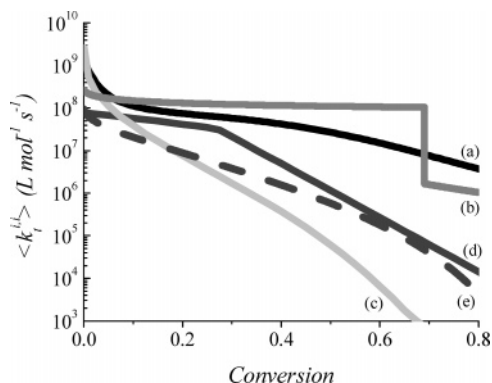


Figure 7. Comparison between various model predictions from literature and experimental data for the chain length dependent termination rate coefficients ($\langle k_t^{i,i} \rangle$) vs fraction conversion (x). Curves: (a) experimental $\langle k_t^{i,i} \rangle$ determined from the RAFT-mediated polymerization of methyl methacrylate (MMA) in bulk at 80 °C initiated with azobis(isobutyronitrile) (AIBN); (b) prediction using the Mahabadi and O'Driscoll approach;^{23,61} (c) prediction using the Russell and Gilbert approach;^{68,73,74} (d) prediction using the Peklak approach;⁷⁶ (e) prediction using the Ross and Laurence approach.⁷⁵

determined $k_t^{i,j}$ (for termination between two propagating radicals of different chain lengths i and j) from an average (via either a geometric, harmonic or diffusion mean) of $k_t^{i,i}$ and $k_t^{j,j}$. Obviously, as these models cannot directly access $k_t^{i,i}$ or $k_t^{j,j}$ they use adjustable parameters to provide a fit with their rate and molecular weight data. These include approaches proposed by Mahabadi and O'Driscoll,^{23,40,61–64} Gilbert and Russell,^{65–74} and Ross and Laurence⁷⁵ as well as Peklak et al.⁷⁶ (who studied the RAFT-mediated polymerization of MMA in the gel regime). The Supporting Information section briefly summarizes each model and provides the relevant parameters used to compare these approaches to our RAFT-mediated data.

Figure 7 shows the comparison between the $k_t^{i,i}(x)$ values predicted by each of these models and the $k_t^{i,i}(x)$ values extracted from the surface profile of Figure 2 for the RAFT-mediated polymerization carried out using 50 mM RAFT agent at 80 °C. It should be noted that some parameters could not be obtained at 80 °C, and therefore we may not have used the optimum values. However, we believe that the variation in the parameters would not significantly change the fit with the experimental $k_t^{i,i}(x)$. While the model of Mahabadi and O'Driscoll provides the best agreement with $k_t^{i,i}(x)$, all the models studied provide less than satisfactory agreement particularly in the gel regime. It is encouraging that the models of Gilbert and Russell and Mahabadi and O'Driscoll were successful in predicting the dilute regions of the $k_t^{i,i}(x)$ profile. Interestingly, both these approaches use the Smoluchowski model in this region which has been shown to agree with termination data for small radical reactions.⁷⁷

Conclusions

The termination rate coefficient, $k_t^{i,i}$, for propagating chains of near equal length, i , was evaluated using the RAFT-CLD-T method over a wide range of chain lengths and up to a conversion of 70% for MMA polymerizations carried out in the presence of the RAFT agent, CPDB, at 80 °C. We found that the gel onset corresponded to the conversion at which chain overlap occurred (i.e., c^*) and was found to range from 15 to 30% conversion depending on the M_n . It was further shown that c^* also corresponded with the gel onset conversions for vinyl acetate and methyl acrylate. The chain length dependence of k_t in the gel regime scaled as $\alpha_{\text{gel}}(x) = 1.8x + 0.056$, suggesting that reptation alone does not play a role in our

system. Using the k_t dependencies for chain length and conversion, we constructed a composite model to accurately describe $k_t^{i,i}$ for chain lengths up to 3200 and conversions up to 70%. As the RAFT-CLD-T method allows accurate $k_t^{i,i}$ to be obtained, we compared these termination profiles with various well-known termination models. While the model of Mahabadi and O'Driscoll gave the best agreement with $k_t^{i,i}(x)$, all the models studied proved less than satisfactory, particularly in the gel regime. This model approach can be readily applied to any monomer provided accurate $k_t^{i,i}(x)$ data can be accessed and parameters $k_t^{1,1}$, α_S , i_{SL} , α_L , i_{gel} , and $\alpha_{\text{gel}}(x)$ evaluated.

Acknowledgment. M.J.M, C.B.-K. and M.H.S acknowledge financial support from the Australian Research Council (ARC) in the form of Discovery grants. G.J.-H. acknowledges financial support from the Australian Institute for Nuclear Science and Engineering (PGRS scholarship) and the University of Queensland (UQJRS scholarship). T.P.D. acknowledges receipt of a Federation Fellowship, C.B.-K. acknowledges receipt of an Australian Professorial Fellowship and M.J.M acknowledges receipt of a QEII Fellowship (all ARC fellowships).

Supporting Information Available: Text giving experimental procedures for the synthesis and molecular weight data for MMA RAFT-mediated polymerizations, the $k_t^{i,i}(x)$ surface function, the various termination models, and fits of c^* with gel onset for MA and VAc polymerizations, including a figure showing a plot of the gel onset conversion profiles and tables of time, conversion molecular weight, and dispersion data. This material is available free of charge via the Internet at <http://pubs.acs.org>.

References and Notes

- Shultz, G. V.; Harborth, G. *Angew. Chem.* **1947**, *59*, 90–92.
- Trommsdorf, E.; Kohle, H.; Lagally, P. *Makromol. Chem.* **1948**, *1* (3), 169–198.
- Matheson, M. S.; Auer, E. E.; Bevilacqua, E. B.; Hart, E. J. *J. Am. Chem. Soc.* **1949**, *71*, 497–504.
- Matheson, M. S.; Auer, E. E.; Bevilacqua, E. B.; Hart, E. J. *J. Am. Chem. Soc.* **1951**, *73*, 5395–5400.
- Bogunjoko, J. S. T.; Brooks, B. W. *Makromol. Chem.* **1983**, *184*, 1603–1621.
- Chekal, B. P.; Torkelson, J. M. *Macromolecules* **2002**, *35*, 8126–8138.
- Bauer, B. J.; Fetters, L. J.; Graessley, W. W.; Hadjichristidis, H.; Quack, G. J. *Macromolecules* **1989**, *22*, 2337–2347.
- Lee, H. B.; Turner, D. T. *Macromolecules* **1977**, *10*, 231–235.
- Nwammuo, P. O.; Maitland, G. C. *J. Chem. Soc., Faraday Trans.* **1992**, *88*, 1803–1818.
- Mahabadi, H. K. *Macromolecules* **1985**, *18*, 1319–1330.
- Barner-Kowollik, C.; Buback, M.; Egorov, M.; Fukuda, T.; Goto, A.; Olaj, O. F.; Russell, G. T.; Vana, P.; Yamazoe, H.; Zetterlund, P. B. *Prog. Polym. Sci.* **2005**, *30*, 605–643.
- Vana, P.; Davis, T. P.; Barner-Kowollik, C. *Macromol. Rapid Commun.* **2002**, *23*, 952–956.
- Lovestead, T. M.; Theis, A.; Davis, T. P.; Stenzel, M. H.; Barner-Kowollik, C. *Macromolecules* **2006**, *39*, 4975–4982.
- Theis, A.; Stenzel, M. H.; Davis, T. P.; Barner-Kowollik, C. *ACS Symp. Ser.* **2006**, *944*, 486–500.
- Monteiro, M. J. *J. Polym. Sci., Part A: Polym. Chem.* **2005**, *43*, 3189–3204.
- Theis, A.; Feldermann, A.; Charton, N.; Stenzel, M. H.; Davis, T. P.; Barner-Kowollik, C. *Macromolecules* **2005**, *38*, 2595–2605.
- Theis, A.; Feldermann, A.; Charton, N.; Davis, T. P.; Stenzel, M. H.; Barner-Kowollik, C. *Polymer* **2005**, *46*, 6797–6809.
- Junkers, T.; Theis, A.; Buback, M.; Davis, T. P.; Stenzel, M. H.; Vana, P.; Barner-Kowollik, C. *Macromolecules* **2005**, *38*, 9497–9508.
- Theis, A.; Davis, T. P.; Stenzel, M. H.; Barner-Kowollik, C. *Polymer* **2006**, *47*, 999–1010.
- Johnston-Hall, G.; Theis, A.; Monteiro, M. J.; Davis, T. P.; Stenzel, M. H.; Barner-Kowollik, C. *Macromol. Chem. Phys.* **2005**, *206*, 2047–2053.
- Smith, G. B.; Russell, G. T.; Heuts, J. P. A. *Macromol. Theor. Simul.* **2003**, *12*, 299–314.
- Theis, A.; Davis, T. P.; Stenzel, M. H.; Barner-Kowollik, C. *Macromolecules* **2005**, *38*, 10323–10327.

- (23) Cardenas, J. N.; O'Driscoll, K. *J. Polym. Sci., Part A: Polym. Chem.* **1976**, *14*, 883.
- (24) Balke, S. T.; Hamielec, A. E. *J. Appl. Polym. Sci.* **1973**, *17*, 905–949.
- (25) O'Neil, G. A.; Wisnudel, M. B.; Torkelson, J. M. *Macromolecules* **1996**, *29*, 7477–7490.
- (26) Johnston-Hall, G.; Monteiro, M. J. Manuscript in preparation.
- (27) Malavasic, T.; Vizovisek, I.; Lapanje, S.; Moze, A. *Makromol. Chem.* **1973**, *175*, 873–880.
- (28) Chong, B. Y. K.; Krstina, J.; Le, T. P. T.; Moad, G.; Postma, A.; Rizzardo, E.; Thang, S. H. *Macromolecules* **2003**, *36*, 2256–2272.
- (29) Monteiro, M. J.; de Brouwer, H. *Macromolecules* **2001**, *34*, 349–352.
- (30) Kwak, Y.; Goto, A.; Tsujii, Y.; Murata, Y.; Komatsu, K.; Fukuda, T. *Macromolecules* **2002**, *35*, 3026–3029.
- (31) Kwak, Y.; Goto, A.; Fukuda, T. *Macromolecules* **2004**, *37*, 1219–1225.
- (32) Chernikova, E.; Morozov, A.; Leonova, E.; Garina, E.; Golubev, V.; Bui, C.; Charleux, B. *Macromolecules* **2004**, *37*, 6329–6339.
- (33) Coote, M. L.; Radom, L. *J. Am. Chem. Soc.* **2003**, *125*, 1490–1491.
- (34) Barner-Kowollik, C.; Coote, M. L.; Davis, T. P.; Radom, L.; Vana, P. *J. Polym. Sci., Part A: Polym. Chem.* **2003**, *41*, 2828–2832.
- (35) Feldermann, A.; Coote, M. L.; Stenzel, M. H.; Davis, T. P.; Barner-Kowollik, C. *J. Am. Chem. Soc.* **2004**, *126*, 15915–15923.
- (36) Moad, G.; Rizzardo, E.; Thang, S. H. *Aust. J. Chem.* **2005**, *58*, 379–410.
- (37) North, A.; M.; Reed, G. A. *J. Polym. Sci.* **1963**, *A1*, 1311–1321.
- (38) Plate, N. A.; Pomarenko, A. G. *Polym. Sci. USSR* **1974**, *16*, 3067.
- (39) Horie, K.; Mita, I.; Kambe, H. *J. Polym. Sci., Part A: Polym. Chem.* **1968**, *6*, 2663–2676.
- (40) Dionisio, J.; Mahabadi, H. K.; O'Driscoll, K.; Abuin, E.; Lissi, E. A. *J. Polym. Sci., Part A: Polym. Chem.* **1979**, *17*, 1891–1900.
- (41) O'Driscoll, K. *J. Pure Appl. Chem.* **1981**, *53*, 617–626.
- (42) Bueche, F. *Physical Properties of Polymers*; Interscience: New York, 1962.
- (43) Onogi, S.; Kobayashi, T.; Kojima, Y.; Taniguchi, Y. *J. Appl. Polym. Sci.* **1963**, *7*, 847–859.
- (44) Cornet, C. F. *Polymer* **1965**, *6*, 373–384.
- (45) Graessley, W. W. *The Entanglement Concept in Polymer Rheology*; Springer-Verlag: New York, 1974; p 1.
- (46) Turner, D. T. *Macromolecules* **1977**, *10*, 221–225.
- (47) Lee, H. B.; Turner, D. T. *Macromolecules* **1977**, *10*, 226–231.
- (48) High, K. A.; Lee, H. B.; Turner, D. T. *Macromolecules* **1979**, *12*, 332–337.
- (49) Lee, H. B.; Turner, D. T. *Polym. Prepr. (Am. Chem. Soc., Div. Polym. Chem.)* **1978**, *19*, 603–605.
- (50) Tulig, T. J.; Tirrell, M. *Macromolecules* **1981**, *14*, 1501–1511.
- (51) Tulig, T. J.; Tirrell, M. *Macromolecules* **1982**, *15*, 459–463.
- (52) Lachinov, M. B.; Simonian, A.; Georgieva, T. G.; Zubov, V. P.; Kabanov, V. A. *J. Polym. Sci.: Polym. Chem. Ed.* **1978**, *17*, 613–616.
- (53) Abuin, E.; Lissi, E. A. *J. Macromol. Sci. Chem.* **1977**, *A11*, 287–294.
- (54) Cotton, J. P.; Nierlich, M.; Boue, F.; Daoud, M.; Farnoux, B.; Jannink, G.; Duplessix, R.; Picot, C. *J. Chem. Phys.* **1976**, *65*, 1101–1108.
- (55) Lodge, T. P.; Muthukumar, M. *J. Phys. Chem.* **1996**, *100*, 13275–13292.
- (56) Bovey, F. A. *Chain Structure and Conformation of Macromolecules*. Academic Press: New York, 1982.
- (57) Dondos, A.; Papanagopoulos, D. *Colloid Polym. Sci.* **1996**, *274*, 634–639.
- (58) Wang, X.; Ruckenstein, E. *J. Appl. Polym. Sci.* **1993**, *49*, 2179–2188.
- (59) De Gennes, P. G. *J. Chem. Phys.* **1971**, *55*, 572.
- (60) Piton, M. C.; Gilbert, R. G.; Chapman, B. E.; Kuchel, P. W. *Macromolecules* **1993**, *26*, 4472–4477.
- (61) Mahabadi, H. K.; O'Driscoll, K. *J. Polym. Sci.: Polym. Chem. Ed.* **1977**, *15*, 283–300.
- (62) O'Driscoll, K. *Makromol. Chem.* **1977**, *178*, 899–903.
- (63) Mahabadi, H. K.; O'Driscoll, K. *J. Polym. Sci., Polym. Lett. Ed.* **1976**, *14*, 671–673.
- (64) O'Driscoll, K. *Makromol. Chem.* **1979**, *180*, 2053–2056.
- (65) Russell, G. T.; Napper, D. H.; Gilbert, R. G. *Macromolecules* **1988**, *21*, 2141–2148.
- (66) Russell, G. T.; Gilbert, R. G.; Napper, D. H. *Macromolecules* **1992**, *25*, 2459–2469.
- (67) Buback, M.; Huckestein, B.; Kuchta, F.-D.; Russell, G. T.; Schmidt, A. D. *Macromol. Chem. Phys.* **1994**, *195*, 2117–2140.
- (68) Russell, G. T. *Macromol. Theor. Simul.* **1994**, *3*, 439–468.
- (69) Buback, M.; Gilbert, R. G.; Hutchinson, R. A.; Klumpermann, B.; Kutcha, F.-D.; Manders, B. G.; O'Driscoll, K.; Russell, G. T.; Schweer, J. *Macromol. Chem. Phys.* **1995**, *196*, 3267–3280.
- (70) Russell, G. T. *Macromol. Theor. Simul.* **1995**, *4*, 497–517.
- (71) Russell, G. T. *Macromol. Theor. Simul.* **1995**, *4*, 519–548.
- (72) Russell, G. T. *Macromol. Theor. Simul.* **1995**, *4*, 549–576.
- (73) Gilbert, R. G. *Emulsion Polymerization: A Mechanistic Approach*. 1st Ed.; Academic Press: London, 1995; p 362.
- (74) Russell, G. T.; Napper, D. H.; Gilbert, R. G. *Macromolecules* **1992**, *25*, 2459–2469.
- (75) Ross, R. T.; Laurence, R. L. *AIChE Symp. Ser.* **1976**, *160*, 74–79.
- (76) Peklak, D. A.; Butte, A.; Storti, G.; Morbidelli, M. *J. Polym. Sci., Part A: Polym. Chem.* **2006**, *44*, 1071–1085.
- (77) Fischer, H.; Paul, H. *Acc. Chem. Res.* **1987**, *20*, 200–206.
- (78) Beuermann, S.; Buback, M.; Davis, T. P.; Gilbert, R. G.; Hutchison, R. A.; Friedrich, O. O.; Russell, G. T.; Heuts, J. P. A.; van Herk, A. M. *Macromol. Chem. Phys.* **2003**, *198*, 1545–1560.
- (79) Brandup, J.; Immergut, E. H.; Grulke, E. A. *Polymer Handbook*; J. Wiley & Sons: New York, 1989.
- (80) Sperling, L. H. *Introduction to Physical Polymer Science*, 3rd ed.; John Wiley & Sons: New York, 2001.
- (81) Stickler, M.; Panke, D.; Wunderlich, W. *Makromol. Chem.* **1987**, *188*, 2651–2664.
- (82) De Gennes, P. G. *Scaling Concepts in Polymer Physics*; Cornell University Press: Ithaca, NY, 1979.
- (83) Griffiths, M. C.; Strauch, J.; Monteiro, M. J.; Gilbert, R. G. *Macromolecules* **1998**, *31*, 7835–7844.
- (84) De Gennes, P. G. *Macromolecules* **1976**, *9*, 572–593.
- (85) De Gennes, P. G. *Macromolecules* **1976**, *9*, 594–598.
- (86) Ying, Q.; Chu, B. *Macromolecules* **1987**, *20*, 362–366.
- (87) Tamai, Y.; Konishi, T.; Einaga, Y.; Fujii, M.; Yamakawa, H. *Macromolecules* **1990**, *23*, 4067–4075.
- (88) De Gennes, P. G.; Leger, L. *Annu. Rev. Phys. Chem.* **1982**, *33*, 49–61.